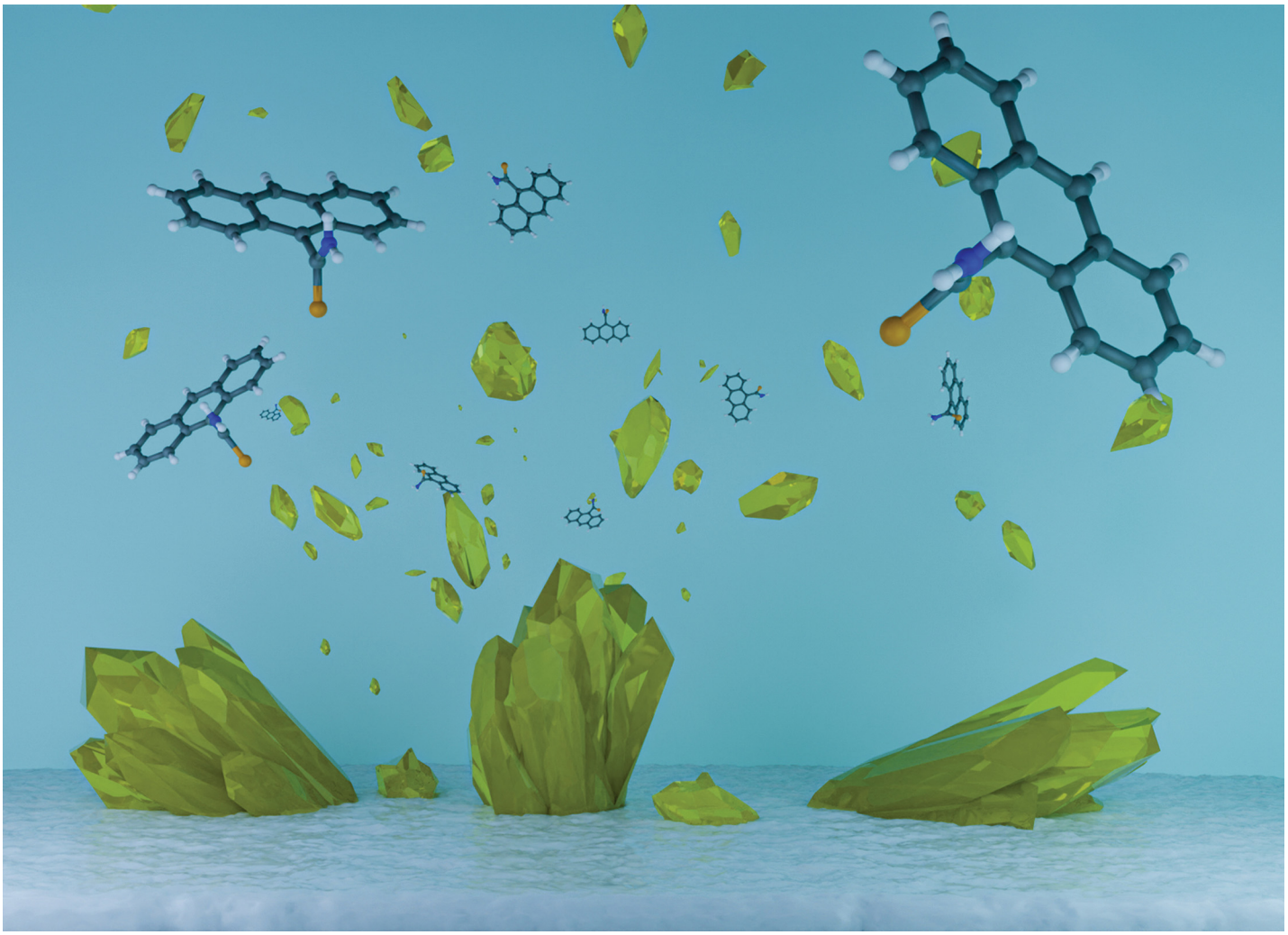

Showcasing research from Professor Hutchins' laboratory, Department of Chemistry and MU Materials Science & Engineering Institute, University of Missouri, Columbia, Missouri, United States. Image designed and illustrated by Matthew J. Walker.

Off-the-shelf thermosalience of anthracene-9-thiocarboxamide

The thermosalient behavior of anthracene-9-thiocarboxamide is demonstrated, and crystals of the material spontaneously fracture and jump upon cooling. A combination of hydrogen bonds and pi stacking interactions sustain the solid. Uniaxial negative and biaxial positive thermal expansion precede thermosalience.

As featured in:

See Kristin M. Hutchins *et al.*, *Chem. Commun.*, 2024, **60**, 7697.

ROYAL SOCIETY OF CHEMISTRY

rsc.li/chemcomm

Registered charity number: 207890

ChemComm

COMMUNICATION

View Article Online
View Journal | View Issue

Cite this: *Chem. Commun.*, 2024, **60**, 7697

Received 14th April 2024,
Accepted 22nd May 2024

DOI: 10.1039/d4cc01765j

rsc.li/chemcomm

Off-the-shelf thermosalience of anthracene-9-thiocarboxamide†

Gary C. George III, [a] Samantha J. Kruse, [b] Tori Z. Forbes [b] and Kristin M. Hutchins *[ac]

We demonstrate thermosalient behavior in anthracene-9-thiocarboxamide. Upon cooling, the crystalline material spontaneously fractures and jumps. Strong anisotropic thermal expansion precedes thermosalience, and the combination of hydrogen bonds and weaker interlayer interactions affords the macroscopic response. By incorporating structural moieties from different classes of thermosalient solids and using an underexplored supramolecular synthon, a dynamic, multifunctional material is achieved.

Crystalline materials that exhibit dynamic behaviors have recently begun to emerge. Although crystalline solids are frequently associated with being hard and rigid materials, recent work has demonstrated that molecular crystals can be relatively 'soft' materials, undergoing bending, ratchet or gear-like motion,[1] and salient effects.[2] Thermosalience is one such interesting behavior that has been discovered in a limited number of crystalline materials including both single- and multi-component crystals.[3] Thermosalience occurs when crystals leap or jump in response to undergoing a first-order phase transition that is triggered by a change in temperature. The driving force for thermosalience varies between materials and can be caused by several structural perturbations.[4] This macroscopic response to temperature gives way to a range of dynamic, responsive materials, including thermal sensors and actuators.[5] For example, metal-coated thermosalient compounds have been used as electrical fuses, wherein a change in temperature causes thermosalience and the circuit breaks.[6] Photosalience is a related property wherein crystals undergo salient effects in response to light. A few materials have been shown to exhibit both thermosalience and photosalience.[7]

Although the number of crystals that exhibit salient properties has grown over the last five years, understanding and predicting the structural features, intermolecular forces, and mechanisms that will afford salient properties in a given compound remains challenging. Here, we describe the thermosalient behavior of anthracene-9-thiocarboxamide (AnThio, Fig. 1a) and demonstrate strong anisotropic thermal expansion (uniaxial negative and biaxial positive) occurs prior to the salient effect. Structurally, AnThio contains two key chemical moieties, one commonly seen in Class I thermosalient solids,[4] the rigid anthracene ring system, and the other similar to those

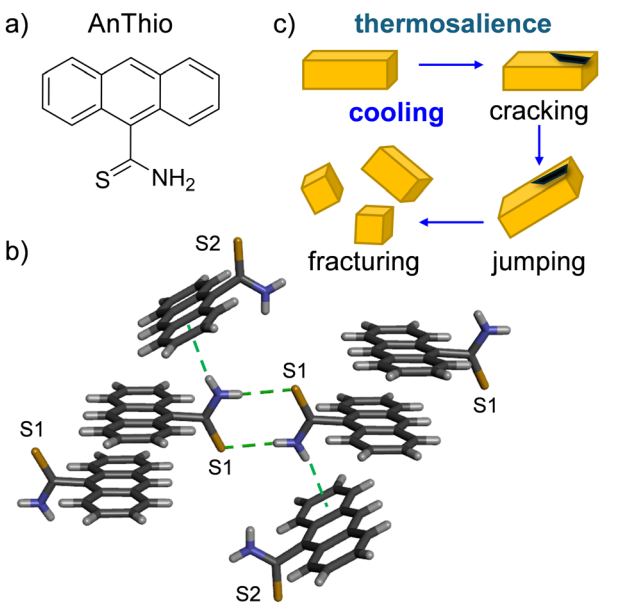

Fig. 1 AnThio: (a) chemical structure, (b) X-ray crystal structure and packing at 300 K highlighting two crystallographically unique AnThio molecules (S1 or S2), and (c) schematic of thermosalience. Hydrogen bonds shown with green dashed lines.

[a] *Department of Chemistry, University of Missouri, Columbia, Missouri 65211, USA. E-mail: kristin.hutchins@missouri.edu*
[b] *Department of Chemistry, University of Iowa, Iowa City, Iowa 52242, USA*
[c] *MU Materials Science & Engineering Institute, University of Missouri, Columbia, Missouri 65211, USA*

† Electronic supplementary information (ESI) available: Experimental details, X-ray diffraction data, thermal expansion analysis, DSC, PXRD patterns, and images and videos of thermosalient events. CCDC 2347862–2347868. For ESI and crystallographic data in CIF or other electronic format see DOI: https://doi.org/10.1039/d4cc01765j

in Class III solids, the hydrogen bond donor/acceptor thiocarboxamide. Given the presence of the thiocarboxamide group, the solid is best described as a Class III thermosalient material and the transition involves sliding of anthracene layers. Neighboring layers undergo opposite types of expansion, *i.e.* negative or positive, while the inter-layer direction undergoes significant positive expansion before the thermosalience. Thiocarboxamide functional groups are structurally analogous to carboxylic acids and amides; however, they have been significantly less explored in the context of supramolecular chemistry. Thermosalient molecules in Class III often contain carboxylic acid, amide, phenol, or amine groups, but, to our knowledge, this is the first molecule containing a thiocarboxamide functional group to exhibit thermosalience.

AnThio is commercially available; however, the crystal structure was not reported until recently by our group (Fig. 1b).[8] In the prior work, we demonstrated the photoreactivity of AnThio, which underwent a [4+4] cycloaddition reaction in the solid state. Our ongoing interest in thermal expansion properties of organic solids led us to investigate the behavior of AnThio in response to temperature change.

Commercial AnThio was recrystallized from ethyl acetate to obtain higher quality single crystals for variable temperature single-crystal X-ray diffraction (SCXRD) experiments. During initial attempts to collect SCXRD data at 100 K, the single crystal of AnThio would either disappear from the mounting loop or would diffract as if it were polycrystalline. Therefore, single crystals of AnThio were instead mounted at 300 K, and the crystals remained intact. SCXRD experiments were conducted over the temperature range of 300–160 K in increments of 20 K and full data sets were acquired.

As previously reported,[8] at 300 K, AnThio lies in the triclinic space group $P\bar{1}$ with unit cell axes lengths of 9.30, 9.90, and 13.27 Å for the *a*, *b*, and *c* axes, respectively. The asymmetric unit contains two unique AnThio molecules, with sulfur atoms labeled S1 or S2. The AnThio molecules interact through centrosymmetric thiocarboxamide dimers, and the second N–H group engages in an N–H$\cdots\pi$ interaction (Fig. 1b). The dimers contain identical thiocarboxamide groups (S1 or S2), while the second N–H group interacts with a crystallographically different AnThio molecule. The anthracene moieties also self-assemble into discrete π-stacked pairs and the thiocarboxamide groups are oriented on opposite sides. AnThio maintains this triclinic space group, unit cell, and general packing arrangement from 300 K to 160 K (Tables S1 and S2, Fig. S1–S3, ESI†).

When AnThio was cooled below 160 K, the crystal fragments, and neither the unit cell dimensions, nor crystal structure were able to be determined (even when mounted with epoxy). To gain insight into this potential thermosalient behavior, the thermal expansion coefficients and structural changes were investigated. Indeed, anomalous, colossal, and/or anisotropic thermal expansion directly before thermosalient events have been previously observed in other systems.[9]

Between 300–160 K, AnThio undergoes positive thermal expansion along the *a* and *c* axes, and the axes lengths decreased by 1.3% and 0.9%, respectively. However, over the same temperature range, AnThio undergoes negative thermal expansion along the *b* axis, and the length increased by 0.3%. The α and β angles decrease linearly with temperature; however, the γ angle behaves non-linearly (Fig. S4, ESI†).

The variable-temperature experiment includes data at eight temperatures in total. When examining the data in the upper (240–300 K) and lower (160–220 K) temperature regions, most of the changes in the unit cell parameters are similar; however, two exceptions are notable. Between 300–240 K, the *b*-axis length increases by 0.017 Å, but the length increases by only half as much between 220–160 K (0.008 Å). The non-linear behavior of the γ angle occurs in the lower temperature region.

The thermal expansion coefficients for AnThio were calculated for the entire temperature range (160–300 K), as well as the upper and lower temperature ranges, 240–300 K and 160–220 K, respectively. Due to the triclinic system, PASCal[10] was used to calculate the principal axes (X_1, X_2, and X_3) and linear thermal expansion coefficients (α_{X_1}, α_{X_2}, and α_{X_3}) for each temperature range (Table 1 and Fig. S5–S7, ESI†).

Regardless of the temperature range, AnThio exhibits negative expansion along the X_1 direction, moderate positive expansion in the X_2 direction, and colossal (or near-colossal) positive expansion in the X_3 direction and volumetrically. Interestingly, the directions of principal axes X_2 and X_3 switch between the upper and lower temperature ranges, *i.e.*, as the thermosalient transition is approached (Fig. S8, ESI†).

The direction of the X_1 axis encompasses primarily the crystallographic *b* axis, which undergoes negative thermal expansion. The *b* axis is dominated by layers of hydrogen-bonded dimers and π-stacked AnThio molecules containing S1. The distance between neighboring S1 AnThio molecules increases upon cooling, affording the negative expansion (Fig. 2a, blue). The degree of negative expansion is larger in the high temperature region because this distance increases by *ca.* two times as much when compared to the low temperature region.

The directions of X_2 and X_3 are switched in the upper and lower temperature regions. In the low temperature region, the X_2 direction encompasses primarily changes in the crystallographic *a* axis. This direction is dominated by layers of hydrogen-bonded dimers and π-stacked AnThio molecules containing S2.

Table 1 Thermal expansion coefficients for AnThio within different temperature ranges. The errors are in parentheses and the approximate crystallographic axes are in brackets

Temperature range	α_{X_1} (MK^{-1}) [axis]	α_{X_2} (MK^{-1}) [axis]	α_{X_3} (MK^{-1}) [axis]	α_V (MK^{-1})
160–300 K	−27 (2) [−1 7 1]	74 (1) [3 −1 2]	102 (3) [5 1 −3]	151 (2)
240–300 K (upper range)	−34 (1) [0 4 1]	72 (1) [1 −2 4]	120 (3) [4 0 −1]	159 (3)
160–220 K (lower range)	−17 (2) [−1 7 1]	69 (1) [6 −1 2]	90 (1) [−3 −1 4]	142 (1)

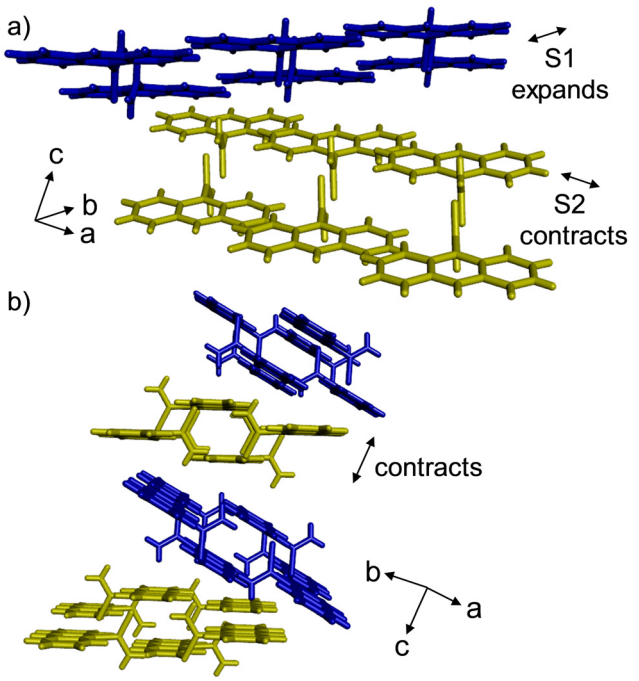

Fig. 2 X-ray crystal structure packing of AnThio showing (a) simultaneous expansion and contraction of neighboring moieties and (b) overall contraction in the π-stacked direction upon cooling. AnThio molecules containing S1 are in blue and S2 are in yellow.

The distance between the neighboring S2 AnThio molecules decreases upon cooling, affording the positive expansion (Fig. 2a, yellow). In the low temperature region, the X_3 direction is dominated by changes in the π stacking and N–H···π interactions between the layers of AnThio molecules (Fig. 2b). The distance between the anthracene molecules in adjacent layers, as well as the N–H···π separations decrease upon cooling. In the upper temperature range, the X_2 direction includes the N–H···π contacts and π stacking, while the X_3 direction includes the S2 AnThio molecules (Fig. S8–S10, ESI†).

Naumov has outlined three classes of thermosalient solids.[4] Class I includes flat, rigid molecules that pack into layered structures (*e.g.*, pentacene, substituted benzenes), which typically lack strong hydrogen-bonding moieties. Intermolecular interactions in Class I solids are usually weak, and the thermosalient event occurs when strains are larger than the interlayer interactions.[11] AnThio contains an anthracene structural motif, which affords layered packing similar to Class I compounds. However, the presence of the thiocarboxamide motif affords strong hydrogen-bonded dimers, differing from other Class I compounds. Alternatively, Class III thermosalient solids exhibit hydrogen-bonded dimeric or polymeric structures, which are further connected through weak intermolecular forces. The mechanism for thermosalience in Class III materials involves cooperative sliding of the hydrogen-bonded assemblies when the temperature is changed. The strain in the crystal is then converted into the macroscopic mechanical motion. Strong anisotropic thermal expansion has been shown to accompany thermosalience. In the case of AnThio, the layer packing alternates in an S1–S2 fashion (Fig. 2b). The layer containing S1 AnThio molecules exhibits negative expansion, while the layer containing S2 AnThio molecules exhibits positive expansion, which supports the sliding layer mechanism and affords strong anisotropic thermal expansion. At the same time, the stacking direction exhibits large expansion prior to the thermosalient event. Several known thermosalient solids belonging to Class III (thus far) contain two different hydrogen-bond donor groups, based on carboxylic acid, amide, alcohol, or amine groups.[4,9b,11,12] To our knowledge, AnThio is the first Class III thermosalient material that contains a thiocarboxamide functional group.

The thermosalient transition was examined in the bulk using differential scanning calorimetry (DSC). Thermosalient materials often exhibit a ''sawtooth-like'' pattern in the thermogram.[4,12a] The characteristic sawtooth pattern is indeed observed when AnThio is cooled from 25 to −150 °C (298–123 K) and the overall enthalpy is comparable to other solids. A slight hysteresis of the temperature at which thermosalience occurs is seen in the thermogram when compared to the SCXRD data (Fig. 3). The thermogram recorded using the commercial source exhibits a broader signal, while the recrystallized sample exhibits sharp peaks (Fig. S11–S14, ESI†). Notably, the crystals are larger in size after recrystallization than from the commercial source. Transitions in DSC can exhibit broader signals using a uniform powder, rather than individual single crystals.[13]

To characterize the low temperature phase present after the thermosalient event, variable temperature powder X-ray diffraction (PXRD) was used, as crystals are unsuitable for SCXRD after thermosalience. Data was collected at room temperature and 173 K (−100 °C), and the low temperature data showed the emergence of a new phase (Fig. 4). At low temperature, some material remained in the room temperature phase, which did not allow for adequate indexing and structure solution. Grinding thermosalient crystals can reduce the ability of the crystal to accumulate strain and exhibit the thermosalient transition.[2] The powder pattern does demonstrate formation of a new crystalline phase, which confirms the first-order phase transition.[11] Given the rapid response of single crystals to flash

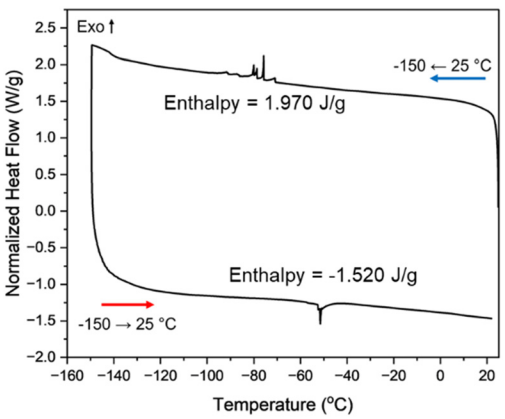

Fig. 3 DSC thermogram of AnThio recrystallized from ethyl acetate. The sharp peak upon cooling is at −76 °C (197 K). A reversible transition is observed upon heating.

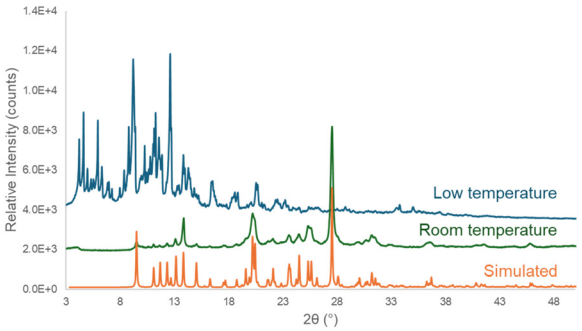

Fig. 4 PXRD data for AnThio: simulated from SCXRD structure at 300 K, collected at room temperature, and collected at low temperature (173 K/−100 °C). The simulated pattern has been shifted by 0.32° to align with experimental data.

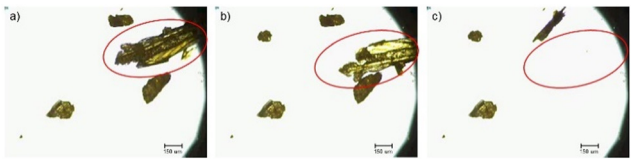

Fig. 5 Still images taken from a video recorded of AnThio during a variable-temperature experiment on a microscope (Video S2, ESI†). AnThio crystals are recrystallized material (a) before, (b) during, and (c) after thermosalience. Scale bars are 150 μm.

cooling in liquid nitrogen, a crystalline powder of AnThio (recrystallized or commercial source) was placed in a vial and submerged in liquid nitrogen for a period of *ca.* 5 min. The vial was removed from liquid nitrogen and a PXRD pattern of the solid was obtained, which demonstrated the material returns to the room temperature phase after exposure to low temperature (Fig. S17, ESI†) in agreement with the DSC data.

The thermosalient phenomenon was recorded in real time using an optical microscope equipped with a camera and variable-temperature stage. Both the commercial material and recrystallized solid exhibited thermosalience through a range of temperatures once the material had reached *ca.* 170 K (Fig. 5, Fig. S18 and S19, Videos S1 and S2, ESI†). Several thermosalient crystals were observed with both samples, with varying degrees of intensity in the explosive event. Larger-sized crystals afforded more intense thermosalient events.[2,14]

Given the thermosalience and established solid-state [4+4] reactivity of AnThio, we exposed single crystals of AnThio to UV irradiation using a variety of UV and visible light sources (254, 300, 350, and 419 nm). The crystals exhibited decreased crystallinity as they underwent the [4+4] cycloaddition reaction but photosalient behavior was not observed. Thus, depending on the applied external stimulus (temperature or light), AnThio exhibits a unique solid-state response (salient or reactive).

Here, we described the thermosalient behavior of a thiocarboxamide-functionalized anthracene, AnThio. The title compound contains structural features that are common in Class I (flat, rigid) and Class III (hydrogen-bond forming) thermosalient solids but was identified to align more closely with Class III due to presence of the hydrogen-bonding thiocarboxamide group. Strong anisotropic expansion occurs prior to the thermosalient transition with negative or positive expansion occurring in alternating layers, accompanied by near colossal positive expansion between layers. DSC and PXRD support thermosalient behavior in the bulk solid. Thermosalient events were also visualized using variable-temperature optical microscopy with larger crystals exhibiting more energetic jumping. AnThio exhibits a salient response to temperature and undergoes a solid-state cycloaddition without salient effects when exposed to UV irradiation, thus, behaving as a dynamic and multi-functional solid. Overall, we envision the combination of structural motifs that support independent solid-state behaviors, as discussed here, will lead to development of new multi-responsive solid-state materials.

The work was supported by the National Science Foundation (DMR-2411677 to K. M. H.). The authors acknowledge Prof. Tomče Runčevski, Lida Aeindartehran, and Nathan Taton for collecting the low temperature PXRD data.

Conflicts of interest

There are no conflicts to declare.

Notes and references

1 L. Zhu, R. O. Al-Kaysi and C. J. Bardeen, *Angew. Chem., Int. Ed.*, 2016, **55**, 7073–7076; D.-D. Han, Y.-L. Zhang, J.-N. Ma, Y.-Q. Liu, B. Han and H.-B. Sun, *Adv. Mater.*, 2016, **28**, 8328–8343.
2 P. Commins, I. T. Desta, D. P. Karothu, M. K. Panda and P. Naumov, *Chem. Commun.*, 2016, **52**, 13941–13954.
3 M. C. Etter and A. R. Siedle, *J. Am. Chem. Soc.*, 1983, **105**, 641–643; J. Gigg, R. Gigg, S. Payne and R. Conant, *J. Chem. Soc., Perkin Trans. 1*, 1987, 2411–2414; Ž. Skoko, S. Zamir, P. Naumov and J. Bernstein, *J. Am. Chem. Soc.*, 2010, **132**, 14191–14202; S. C. Sahoo, S. B. Sinha, M. S. R. N. Kiran, U. Ramamurty, A. F. Dericioglu, C. M. Reddy and P. Naumov, *J. Am. Chem. Soc.*, 2013, **135**, 13843–13850.
4 S. C. Sahoo, M. K. Panda, N. K. Nath and P. Naumov, *J. Am. Chem. Soc.*, 2013, **135**, 12241–12251.
5 J. M. Halabi, I. Séguy, L. Salvagnac, T. Leïchlé, D. Saya, F. Mathieu, B. Duployer, D. P. Karothu, L. Nicu and P. Naumov, *Cell Rep. Phys. Sci.*, 2022, **3**, 101133; P. Naumov, S. Chizhik, M. K. Panda, N. K. Nath and E. Boldyreva, *Chem. Rev.*, 2015, **115**, 12440–12490.
6 A. Khalil, E. Ahmed and P. Naumov, *Chem. Commun.*, 2017, **53**, 8470–8473.
7 B. B. Rath, M. Gupta and J. J. Vittal, *Chem. Mater.*, 2022, **34**, 178–185; W. M. Awad, D. W. Davies, D. Kitagawa, J. Mahmoud Halabi, M. B. Al-Handawi, I. Tahir, F. Tong, G. Campillo-Alvarado, A. G. Shtukenberg, T. Alkhidir, Y. Hagiwara, M. Almehairbi, L. Lan, S. Hasebe, D. P. Karothu, S. Mohamed, H. Koshima, S. Kobatake, Y. Diao, R. Chandrasekar, H. Zhang, C. C. Sun, C. Bardeen, R. O. Al-Kaysi, B. Kahr and P. Naumov, *Chem. Soc. Rev.*, 2023, **52**, 3098–3169.
8 G. C. George III and K. M. Hutchins, *Chem. – Eur. J.*, 2023, **29**, e202302482.
9 (*a*) M. K. Panda, R. Centore, M. Causà, A. Tuzi, F. Borbone and P. Naumov, *Sci. Rep.*, 2016, **6**, 29610; (*b*) L. O. AlimiD. P. van HeerdenP. LamaV. J. SmithL. J. BarbourChem. Commun.54–6211; (*c*) B. B. Rath, G. Gallo, R. E. Dinnebier and J. J. Vittal, *J. Am. Chem. Soc.*, 2021, **143**, 2088–2096.
10 M. Lertkiattrakul, M. L. Evans and M. J. Cliffe, *J. Open Source Softw.*, 2023, **8**, 5556–5559.
11 Y. Yamanoi, K. Omoto, T. Nakae and M. Nishio, *Soft Crystals: Flexible Response Systems with High Structural Order*, Springer Nature Singapore, 2023, pp. 131–153.
12 (*a*) M. K. Panda, T. Runčevski, A. Husain, R. E. Dinnebier and P. Naumov, *J. Am. Chem. Soc.*, 2015, **137**, 1895–1902; (*b*) S. Mittapalli, P. D. Sravanakumar and A. Nangia, *IUCrJ*, 2017, **4**, 243–250.
13 B. Perrenot and G. Widmann, *Thermochim. Acta*, 1994, **234**, 31–39.
14 A. Khalil, Chunhua T. Hu and P. Naumov, *CrystEngComm*, 2018, **20**, 636–642.

